Critical current densities and flux creep rates in near optimally doped $BaFe_{2-x}Ru_xAs_2$ (x ≈ 0.7) single crystals

N. Haberkorn,[1] Man Jin Eom,[2] Jung Sang You,[2] Jeehoon Kim,[2, 3] and Jun Sung Kim.[2]

[1] Centro Atómico Bariloche, Comisión Nacional de Energía Atómica. Av. Bustillo 9500, 8400 San Carlos de Bariloche, Argentina.

[2] Department of Physics, Pohang University of Science and Technology, Pohang 790-784, Korea.

[3] CALDES, Institute for Basic Science, Pohang, Korea.

* *e-mail* corresponding author: nhaberk@cab.cnea.gov.ar. Tel : +54 0294 444 5171.

Abstract

We present an investigation of the critical current densities J_c and flux creep rates in a near optimally doped $BaFe_{2-x}Ru_xAs_2$ (x ≈ 0.7) single crystal by (measuring magnetization). The superconducting critical temperature is 18 K. The in-field dependences of the critical current density J_c are due to a mixed pinning scenario produced mainly by large precipitates and a less significant contribution of random disorder. Furthermore, a Maley analysis in the regime dominated by strong pinning centers ($\mu_0 H$ = 0.1 T) is well described through a glassy exponent μ = 1.9 and a collective pinning energy (U_0) smaller than 100 K.

Keywords

A. Superconductors

B. Flux pinning and creep.

1. Introduction

Vortex dynamics in the so-called 122 iron-based superconductors has been the focus of many studies during the last years [1, 2, 3]. Superconductivity can be induced by substituting the different sites, e.g., for $BaFe_2As_2$ with K (Ba site) [4], Co (Fe site) [5], Ru (Fe site) [6] and P [7]. These compounds show superconducting transition temperatures (T_c) between conventional and cuprate superconductors, low anisotropy ($\gamma \approx 2$), and high upper critical fields H_{c2} (small coherence lengths ξ). The vortex matter in 122 systems shows features in common with those observed in cuprates [1,2,3,8]. Small pinning energies (U_0) and glassy relaxation with characteristic exponent μ similar to those predicted by the collective pinning theory have been reported [1,2,9]. The short ξ usually present in 122 systems is particularly susceptible to pinning due to the vortex interaction with small imperfections of the crystalline structure. The resulting pinning is the non-trivial sum over all the contributions of the different types of crystalline defects. Pristine 122 single crystals usually present precipitates [8], twin boundaries [10], chemical inhomogeneities and random disorder [11]. Noticeable enhancement in the critical current density (J_c) has been reported when including artificial pinning centers such as random point defects and amorphous tracks [3,12,13,14,15]. Combining random point defects and strong pinning centers produces a noticeable improvement of in-field J_c [16]. On the other hand, high J_c values, which are promising for construction of superconducting magnets, have been reported in isovalent $BaFe_2(As_{0.66}P_{0.33})_2$ thin films with nanoparticles [17].

The absolute J_c values and their in-field dependences are given by the interaction of the flux vortices and defects [18]. The resulting vortex dynamics depends on the superconducting material, and on the size, geometry and density of the pinning centers. The effectiveness of the pinning depends primarily on the ratio between ξ and the size of the defects, since it is the smallest length scale resolvable by the vortex core [18]. Pinning from inhomogeneities smaller than ξ is much less effective than that produced by large defects. The resulting vortex dynamics for random point disorder has been explained by the weak collective theory. This theory considers that each single vortex line is pinned by the collective action of many weak point-like pins. The pinning energy results from a competition between the pinning potential and the elastic deformation of the vortices. At low fields (single vortex regime SVR), the vortices weakly interact and a single vortex line is collectively trapped by various pins. When the magnetic field is raised, the vortex-vortex interaction increases and the vortices are trapped as bundles [18]. Experimentally, the resulting mechanisms for vortex pinning in iron-based superconductors are more complex as a consequence of mixed pinning landscapes. The temperature and in-field dependences of J_c are well described by superposed collective and strong pinning regimes [8,19].

To understand the role of intrinsic superconducting parameters on the resulting vortex dynamics it is of great importance to compare the magnetic field – temperature (H-T) vortex phase diagrams of iron-based superconductors with modified doping levels [2]. However, the superconducting properties in 122 systems are very sensitive to doping [20,22]. Inhomogeneities and chemical gradients are usually present in as-grown single crystals [21] and are expected to be higher in non-optimal doped systems [5,20]. Among the different 122 systems, $Ba(Fe_{1-x}Ru_x)_2As_2$ is an isovalent substituted one with a maximum T_c around 20 K [22], which presents a strong competition between superconductivity and antiferromagnetic order. This order is suppressed by increasing the Ru doping and thus, superconductivity occurs at x >0.4 [22]. The optimal doped $Ba(Fe_{1-x}Ru_x)_2As_2$ (x ≈ 0.7) has a lower upper critical field (H_{c2}) than other superconducting optimal doped 122 compounds [23,24,25,26,27]. Therefore, it is special for investigating the interaction of large ξ (0) ≈ 4 nm with the mix pinning landscape usually present in as -grown single crystals [9,12,14].

Here, we examine the resulting J_c and vortex dynamics in an as-grown near optimally doped $BaFe_{2-x}Ru_xAs_2$ (x ≈ 0.7) single crystal. We find that the resulting temperature dependence of J_c is well explained by the combination of random point defects and strong pinning centers. Furthermore, collective creep regime (usually manifested as a SPM) is strongly suppressed. This fact can be attributed to the large coherence length ξ (0) ≈ 4 nm, which reduces the pinning produced by random disorder. For fields where pinning is mainly dominated by strong centers ($\mu_0 H$ = 0.1 T), the vortex dynamics is well described by collective pinning theory with a glassy exponent $\mu \approx 1.9$ and a pinning energy (U_0) smaller than 100 K.

2. Material and methods

The single crystals were grown using the self-flux method [22]. Magnetization measurements were performed in a commercial superconducting quantum interference device (SQUID) magnetometer. Lower critical fields (H_{c1}) were determined using SQUID magnetometry. The initial magnetization M (H) was measured at desired temperatures after zero-field cooling of the crystal from above T_c. The critical current density was estimated by applying the Bean critical-state model to the magnetization data, obtained in hysteresis loops, which led to $J_c = \frac{20\Delta M}{dw^2(l - {}^{w}/_{3})}$, where ΔM is the difference in magnetization between the upper and lower branches of the hysteresis loop, and d (0.03 mm), w (0.7 mm), and l (0.8 mm) are the thickness, width, and length of the sample ($l > w$), respectively. The flux creep rate $S = -\frac{d(\ln J_c)}{d\ (\ln t)}$, was recorded over one-hour periods. The initial time (t) was adjusted considering the best correlation factor in the log-log fitting of the $J_c(t)$ dependence. The initial critical state for each creep measurement was generated by applying a field variation of $H \approx 4\ H^*$, where H^* is the field for the full-flux penetration [28].

3. Results and discussion

The resulting T_c = 18.0 (0.2) K of the single crystal was determined opposing magnetization and temperature. To estimate some relevant superconducting parameters (such as thermodynamic critical field H_c, Ginzburg number Gi and depairing critical current J_0), we calculated the penetration length (λ) values by measuring the lower critical fields (H_{c1}) at low temperatures. The H_{c1} values obtained by magnetization can be affected by barriers and vortex pinning on the surface. Therefore, this type of measurement provides an upper limit for H_{c1} estimation. For each T, it was possible to identify the field H_{dev}, in which M(H) deviates from its initial linear dependence $M = -\ V4\pi(1-\eta)H$ corresponding to the Meissner state response (perfect diamagnetism), where V is the crystal volume and η is the appropriate demagnetizing factor. The measurements were performed for both **H**//c and **H**//ab. The respective demagnetization factors are $\eta_c \approx 0.9$ and $\eta_{ab} \approx 0.047$. In addition, to confirm that the superconducting volume coincided with the geometry of the sample, the measured slopes of the linear M vs H Meissner response in both orientations were used. To estimate H_{c1}, $H_{c1}(T) = H_{dev}(T)/(1-\eta)$ was considered. Figure 1 shows typical Meissner slopes at 4.5 K and 7.5 for **H**//ab. Similar procedure was performed for **H**//c (H_{dev} is strongly affected by the demagnetization factor). Inset shows percentage departure of the M (H) data from the Meissner slope and the criteria used to determine $H_{dev}(T)$. The H_{c1} values for both magnetic configurations were estimated from $H_{dev}(4.5K)$ and no major variations are expected between 4.5 K and 0 K [29]. The respective H_{c1} with **H**//c and **H**//ab are 155 (15) Oe and 85

(10) Oe, respectively. The λ values were obtained from $H_{c1} \approx \frac{\Phi_0}{4\pi\lambda^2}(\ln\kappa + 0.5)$, where κ = λ / ξ is the Ginzburg-Landau parameter. For the **H**//ab configuration $\lambda^2 = \lambda_{ab} * \lambda_c$ and $\kappa = (\lambda_{ab}\lambda_c/\xi_{ab}\xi_c)^{1/2}$ were used. By employing ξ_{ab} (0) = 3.9 (0.3) nm and ξ_c (0) = 3.1 (0.4) nm [23,24], λ_{ab} (0) = 210 (20) nm and λ_c = 380 (70) nm were obtained. The estimated λ_{ab} (0) value is similar to those found in other 122 systems [29].

To analyze the properties with **H**// c-axis, using $\xi_{ab}(0)$ = 3.9 (0.3) nm and $\lambda^{ab}(0)$ = 210 (20) nm, the thermodynamic critical field $H_c(T=0) = \frac{\Phi_0}{2\sqrt{2}\pi\lambda(0)\xi(0)}$ = 2800 ± 600 Oe is obtained. The resulting value for the theoretical depairing critical current density is $J_0 = cH_c/3\sqrt{6}\pi\lambda$ = 60 (15) MA cm $^{-2}$ (being *c* the speed of light). The strength of thermal fluctuations can be parameterized by using the Ginzburg number $G_i = \frac{1}{2}\left[\frac{\gamma T_c}{H_c^2(0)\xi^3(0)}\right]^2 \approx 5\text{x}10^{-5}$ [18]. To estimate it, γ ≈ 2 [24] was used. The *Gi* obtained is similar to those obtained in other 122 systems [9,12,14,].

The magnetic field dependence of the critical-current density J_c (*H*) for the $BaFe_{2-x}Ru_xAs_2$ (x ≈ 0.7) single crystal was determined by applying the critical-state Bean model to the magnetization data (obtained from hysteresis loops). Figures 2*a-b* (left y-axis) show the results obtained at 2 K, 5 K, 7.5 K, 10 K and 12.5 K. The self-field J_c at 2 K is around 0.14 MA cm^{-2}, which represents ≈ 0.23 % of the J_0 (*T*=0). The J_c (*H*) dependences obtained at the different temperatures display a modulation that can be associated with different vortex regimes. In the regime I (small fields), the J_c (*H*) dependence is ≈ constant. This regime is usually associated with single vortex pinning, but it can also be affected by self-field effects and geometrical barriers [30]. For regime II (middle fields) J_c (*H*) is well described by a power-law regime ($J_c \propto H^{-\alpha}$), which is observed as a linear dependence on the *log-log* plot. Regime III is evidenced as a modulation in J_c as *H* increases, and it can be associated with collective pinning by vortex bundles [8, 31]. Finally for regime IV, the J_c (*H*) curves present an inflexion point and a fast drop in J_c. This regime can be associated with fast flux creep rates and is usually described as plastic creep [1]. Regime II presents an α = 0.47 for all the temperatures. An α value = 0.55 has been theoretically predicted for pinning for NPs [32]. The α value usually decreases to values as low as 0.2 for samples with CD [33]. Intermediate values between 0.2 and 0.55 can be expected from mixed pinning landscapes produced by extended defects and nanoparticles. Regime III, related to collective pinning, appears as a change of the slope and, at low temperatures, shows a smoother J_c (H) dependence than regime II. A second peak in the magnetization (SPM), known as fishtail effect, is not observed. The J_c (H) curves in $BaFe_{2-x}Ru_xAs_2$ (x ≈ 0.7) are similar to those found in optimally doped $BaFe_{2-x}Co_xAs_2$ single crystals above 20 K [1,2,12]. The SPM (when present) usually disappears at $T \rightarrow T_c$ and is weakly observed in iron arsenide superconductors with larger ξ than those found in optimal doped compounds [12,34]. Moreover, the SPM is gradually suppressed by thermal annealing of the crystals, which indicates that it can be associated with pinning by inhomogeneities in the nanoscale [14].

The S (H) dependences at the different temperatures are shown in Figs. 2*ab* (right y-axis). Regimes II and III at $T \leq 10$ K present a smooth $S(H) < 0.02$. Finally, the S values at regime IV strongly increase [1]. Usually, the S (H) dependences in samples with pinning dominated by random disorder show large change, which is related to the evolution of vortex bundle size [31]. On the other hand, the addition of random point defects and strong pinning centers by irradiation usually enhance J_c, which conceals the regime III [12,14]. Therefore, the resulting vortex dynamics in the $BaFe_{2-x}Ru_xAs_2$ (x ≈ 0.7) single crystals at regimes II and III can be described as a combination of weak collective (due to random point defects) and strong pinning centers (due to a low amount of nanometric inhomogeneities). Moreover, low densities of few weak and strong pinning centers are expected from the low J_c values compared to other 122 systems [12,9,12,14].

A combination of strong and weak pinning centers has been previously observed in other iron based superconductors [8,9,36]. The presence of random point defects can be expected from vacancies and inhomogeneous doping. The presence of strong pinning centers is expected from nanometric phase separation and inhomogeneous doping [35,36]. The vortex pinning produced by a random distribution of particles larger than ξ was discussed in refs. [8,32]. The J_c value in the SVR (low H) produced by nanoparticles can be estimated as $J_c \approx 0.14 n^{1/2}\gamma[DF(T)]^{3/2}J_0$, where n is the density of the pinning particles, D is their diameter (assuming that they are spherical), and $F(T) \approx \ln\left[1 + D^2/8\xi^2(T)\right]$ [32]. To roughly estimate/for practical purposes, $F(T) \sim 1$ can be taken ($D \approx$ a few times ξ). Thus $[DF(T)]^{3/2} \sim (2v)^{1/2}$ is obtained, where v is the volume of one particle, and $J_c \approx 0.14\gamma(2nv)^{1/2}J_0$. Note that nv is the fraction of the volume occupied by the defects. Using adequate superconducting parameters $nv \approx 3.5\text{x}10^5$ is obtained. Assuming spherical pinning centers and D from 12 to 20 nm, we obtain particles densities of $4\text{x}10^{-19}$ m^{-3} and $1\text{x}10^{-18}$ m^{-3}, respectively. These values are very small in comparison with that observed in thin films with very high J_c values [32]. It is worth noting that the α exponent remains approximately constant for the overall range of temperature (from 2 K to 12.5 K). Usually, the α value increases with temperature as a consequence of increments in the fluctuations and vortex-vortex interactions [33]. Excluding thermal fluctuations and as an analogy with correlated disorder, the pinning produced by large defects should be reduced when $\sqrt{2}\xi(T)=D/2$ (with $\xi(T)=\xi(0)(1-T/T_c)^{1/2}$). A crossover from strong to weak pinning is expected at T_{cr} defined by $\frac{T_{cr}}{T_c}=1-\frac{8\xi^2(0)}{D^2}$ [18]. Assuming ξ(0) = 4 nm, D from 12 nm to 20 nm, it is inferred that the strength of the pinning produced by these defects should be systematically reduced when the temperature is increased from 2 to 10 K. The negligible α (T) dependence between 2 K and 12 K indicates that the strong pinning in $BaFe_{2-x}Ru_xAs_2$ (x ≈ 0.7) single crystals should be produced by large sparse non-superconducting regions [35,36].

According to vortex-glass and collective creep theories [18], the effective activation energy as a function of current density (J) is given by $U_{eff}=\frac{U_0(T)}{\mu}\left[\left(\frac{J_c}{J}\right)^{\mu}-1\right]$[eq. 1], where $U_0(T)=U_0G(T)$ is the scale of the pinning energy, U_0 is the collective pinning barrier at T = 0 in the absence of a driving force, G (T) contains the temperature (T) dependence of the superconducting parameters, and μ is the regime-dependent glassy exponent determined by the bundle size and vortex lattice elasticity. For the three-dimensional case and random point defects, the model of the nucleation of vortex loops predicts μ equal to 1/7, 3/2 or 5/2, and 7/9 for SVR, small-bundle (Sb) creep and large-bundle (lb) creep, respectively [18]. From eq. [1], the temperature dependence of the creep rate (S) results in $S=-\frac{d(\ln J)}{d(\ln t)}=\frac{T}{U_0+\mu T\ln(t/t_0)}=\frac{T}{U_0}\left(\frac{J}{J_c}\right)^{\mu}$ [eq. 2], where U_0 is the collective barrier in the absence of a driving force and t_0 is an effective hopping attempt time. According to Maley analysis [37], the effective activation energy $U_{eff}(J)$ can be experimentally obtained considering the approximation in which the current density decays as $\frac{dJ}{dt}=-\left(\frac{J_c}{\tau}\right)e^{-\frac{U_{eff}(J)}{T}}$. The equation for the pinning energy is $U_{eff}=-T\left[ln\left|\frac{dJ}{dt}\right|-C\right]$ [eq. 3], where $C=ln(J_c/\tau)$ is a nominally constant factor. For an overall analysis, it is important to consider the function G (T), which results in $U_{eff}(J,T=0)\approx U_{eff}\,(J,T)/G(T)$. Figure 4$a$ shows the S (T) (left axis) and J_c (T) (right axis) for μ_0H = 0.1 T and **H**//c-axis. This magnetic field was selected considering that regime II includes temperatures from 2K to over 10K. The S (T) dependence shows a plateau from ≈ 6 K to ≈ 11 K ($S \sim 0.018$). Figure 4b shows the respective Maley analysis, $C = 15$ and G (T) were used (see inset Fig. 4b). In the limit of $J << J_c$ the μ exponent can be estimated as $\Delta\ln U(J) / \Delta\ln J$ [38]. The slope at the plateau corresponds to $\mu \approx 1.9$. This value is within the expected for small bundles for random point defects and it has also been observed in cuprates with strong pinning centers [39]. The plateau is well described by $S = (\mu \ln(t/t_0))^{-1} \approx 0.018$ (with $U_0 << \mu T \ln {t}/{t_0}$). Using this approximation and $\mu \approx 1.9$, $\ln(t/t_0) \sim 29$ is obtained, which is in good agreement with previous published values for cuprates [31,38]. The plateau starts at $T \approx 6$ K, indicating that the pinning energy $U_0 < 100$ K [9]. These values are similar to those observed in optimal doped $BaFe_{2-x}Co_xAs_2$ single crystals, which indicates that large defects produce similar vortex dynamics in the different 122 systems [14]. It is worth mentioning that slight changes in the S (H) occur at $T \leq 10$ K when the field is increased from regime II to regime III (see Figs. 2ab). Therefore, small changes in the glassy exponent μ are expected in the regime III. Usually, the vortex dynamics in samples with a SPM (large contribution of random disorder) present a reduction of the S values in the collective regime or regime III [1,2,12,14].

The H-T vortex phase diagram for the $BaFe_{2-x}Ru_xAs_2$ ($x \approx 0.7$) single crystal is shown in Fig. 4 as well as the expected B_2 line obtained from ref. [24]. The crossover between regimes I and II has not been included. At low fields (regime II), J_c (H) is dominated by strong pinning centers. As mentioned above, the power-law regime shows smooth α (T) dependence, which can be related to large defects and weak influence of thermal fluctuations [33]. The crossover line to regime III can be associated with pinning produced by random disorder and strong pinning centers. The elastic interaction of vortices with random pinning potential is displayed as an inflexion on the J_c (H) dependences. Two different regions can be identified in this regime. Below 7.5 K, the J_c (H) curves in the regime III show smoother dependences than in the regime II. Above 7.5 K, the pinning produced by random potential presents poorer in-field dependences than that predicted by the power-law dependence. This fact indicates that the pinning produced by random point defects is strongly suppressed by temperature. Finally, at large fields (regime IV), vortex relaxation is governed by fast creep rates. It has been previously shown that the crossover to fast creep is weakly affected by the inclusion of weak and strong pinning centers [12,14]. The low J_c values (i. e. 0.14 M cm^{-2} at 2 K) compared to other 122 systems, such as $Ba(Fe_{0.925}Co_{0.075})_2As_2$ single crystals (i. e. 0.76 M cm^{-2} at 5 K

[12,14]), indicate that pinning by random disorder and small precipitates is strongly suppressed. This fact can be attributed to the influence of the vortex-defect interaction produced by large ξ, which should be evidenced in the reduction of the effective pinning energy produced by small defects.

4. Summary

In summary, we study the critical current densities J_c and the vortex dynamics in a near optimally doped $BaFe_{2-x}Ru_xAs_2$ ($x \approx 0.7$) single crystal. The data is consistent with mixed pinning scenario produced mainly by large precipitates and a less significant contribution of random disorder. We observe slight changes on the flux creep rates for the range of fields where the pinning is dominated mainly by strong pinning centers (small fields), and for the range of fields where the contribution of collective pinning is evidenced (intermediate fields). The influence of random point defects in the resulting J_c is strongly suppressed by temperature. Furthermore, the Maley analysis in the power-law regime ($\mu_0 H$ = 0.1 T) indicates that the vortex dynamics is well described by a glassy exponent μ similar to that expected in the so-called small bundle regime ($\mu \approx 1.9$), and a collective pinning energy (U_0) smaller than 100 K.

Acknowledgments

The work at POSTECH was supported by NRF through SRC (Grant No. 2011-0030785) program and also by IBS (No. IBSR014-D1-2014-a02). This work also was partially supported by the Institute for Basic Science (IBS) through the Center for Artificial Low Dimensional Electronic Systems by Project Code (IBS-R015-D1). N. H is member of the Instituto de Nanociencia y Nanotecnología (Argentina). N. H. is member of CONICET (Argentina).

Figure 1. Magnetization (*M*) versus magnetic field (*H*) obtained for both **H**//ab after zero-field cooling of the crystal from above T_c to 4.5 K and 7.5 K. Inset: Criteria for H_{dev} determination (Deviation between Meissner slope and experimental).

Figure 2. Magnetic field dependence of the critical current density J_c (left axis) and flux creep rates *S* (right y-axis) with **H** // *c*-axis. *a)* 2 K and 5 K. *b)* 7.5 K, 10 K and 12.5 K.

Figure 3. Temperature dependence of J_c (right axis) and of the flux creep rate *S* (left axis) at $\mu_0 H = 0.1$ T in a $BaFe_{2-x}Ru_xAs_2$ ($x \approx 0.7$) single crystal. *b)* Maley analysis obtained from the data presented in *a)*.The inset shows the *G* (*T*) dependence used for the Maley analysis.

Figure 4. Vortex phase diagram *H-T* in the $BaFe_{2-x}Ru_xAs_2$ ($x \approx 0.7$) single crystal. The B_{c2} line was estimated by considering $\left.{}^{\delta H_{c2}}/_{\delta T}\right|_{T\rightarrow T_c} \approx -1.4$ [24].

[1] R. Prozorov, N. Ni, M.A. Tanatar, V.G. Kogan, R.T. Gordon, C. Martin, E.C. Blomberg, P. Prommapan, J.Q. Yan, S.L. Bud'ko, P.C. Canfield, Phys. Rev. B 78 (2008) 224506-224514.
[2] B. Shen, P. Cheng, Z. Wang, L. Fang, C. Ren, L. Shan, H.H. Wen, Phys. Rev. B 81 (2010) 014503-014514.
[3] Tsuyoshi Tamegai *et al.*, Supercond. Sci. Technol. 25 (2012) 084008-084018.
[4] M. Rotter, M. Tegel, D. Johrendt, Phys. Rev. Lett. 101 (2008) 107006-107010.
[5] A.S. Sefat, R. Jin, M.A. McGuire, B.C. Sales, D.J. Singh, D.Mandrus, Phys. Rev. Lett. 101 (2008) 117004-117008.
[6] A. Thaler, N. Ni, A. Kracher, J.Q. Yan, S.L. Budko, P.C. Canfield, Phys. Rev. B 82 (2010) 014534-014540.
[7] S. Kasahara, T. Shibauchi, K. Hashimoto, K. Ikada, S. Tonegawa, R. Okazaki, H. Shishido, H. Ikeda, H. Takeya, K. Hirata, T. Terashima, Y. Matsuda, Phys. Rev. B 81 (2010) 184519-184523.
[8] C. J. van der Beek *et al.*, Phys. Rev. B 81 (2010) 174517-174527.
[9] N. Haberkorn, M. Miura, B. Maiorov, G.F. Chen, W. Yu, L. Civale, Phys. Rev. B 84 (2011) 094522-094529.
[10] R. Prozorov, M. A. Tanatar, N. Ni, A. Kreyssig, S. Nandi, S.L. Bud'ko, A.I. Goldman, P. Canfield, Phys. Rev. B 80 (2009) 174517-174521.
[11] S. Demirdis, C. J. van der Beek, Y. Fasano, N.R. Cejas Bolecek, H. Pastoriza, D. Colson, F. Rullier-Albenque, Phys. Rev. B 84 (2011) 094517-094514.
[12] N. Haberkorn, B. Maiorov, I.O. Usov, M. Weigand, W. Hirata, S. Miyasaka, S. Tajima, N. Chikumoto, K. Tanabe, Leonardo Civale, Phys. Rev. B 85 (2012) 014522-014529.
[13] Y. Nakajima, Y. Tsuchiya, T. Taen, T. Tamegai, S. Okayasu, M. Sasase, Phys. Rev. B 80 (2009) 012510-012513.
[14] N. Haberkorn, Jeehoon Kim, K. Gofryk, F. Ronning, A.S. Sefat, L. Fang, U. Welp, W.K. Kwok, L. Civale, Supercond. Sci. Technol. 28 (2015) 55011-55018.
[15] T. Taen, F. Ohtake, S. Pyon, T. Tamegai, H. Kitamura, Supercond. Sci. Technol. **28** (2015) 085003-085011.
[16] K. J. Kihlstrom *et al.* Appl. Phys. Lett. **103** (2013) 202601-202604.
[17] M. Miura, *et al.* Nat. Commun. **4** (2013) 2499-2505.
[18] G. Blatter, M.V. Feigel'man, V.B. Geshkenbein, A.I. Larkin, V.M. Vinokur, Rev. Mod. Phys. 66 (1994) 1125-1388.
[19] Yue Sun *et al.* Phys. Rev. B 92 (2015) 144509-144513.
[20] L. Harnagea *et al.*, Phys. Rev. B 83 (2011) 94523-94532.

[21] K. Gofryk, A.B.Vorontsov, I.Vekhter, A.S. Sefat, T. Imai, E.D. Bauer, J.D.Thompson, F. Ronning, Phys.Rev. B 83 (2011) 64513-64516.
[22] M.J. Eom, S.W. Na, C. Hoch, R.K. Kremer, J.S. Kim. Phys. Rev B **85** (2012) 024536-024512.
[23] Xing Jie, Shen Bing, Zeng Bin, Liu JianZhong, Ding XiaXin, Wang ZhiHe, Yang Huan, Wen HaiHu, Sci. China-Phys. Mech. Astron. 55 (2012) 2259-2263.
[24] Youn Jung Jo, Man Jin Eom, Jun Sung Kim, W. Kang. Progress in Superconductivity and Cryogenics 16 (2014) 31-35.
[25] M. Kano, Y. Kohama, D. Graf, F. Balakirev, A.S. Sefat, M.A. McGuire, B.C. Sales, D. Mandrus, S.W. Tozer, J. Phys. Soc. Japan 78 (2009) 84719-84722.
[26] C. Putzke, P. Walmsley, J.D. Fletcher, L. Malone, D. Vignolles, C. Proust, S. Badoux, P. See, H.E. Beere, D. A. Ritchie, S. Kasahara, Y. Mizukami, T. Shibauchi, Y. Matsuda, A. Carrington, Nat. Commun. 5 (2014) 5679-5684.
[27] H.Q. Yuan, J. Singleton, F.F. Balakirev, S.A. Baily, G.F. Chen, J.L. Luo, N.L. Wang, Nature 457 (2009) 565-568.
[28] Y. Yeshurun, A. P. Malozemoff, A. Shaulov, Rev. Mod. Phys. 68 (1996) 911-949.
[29] R.T. Gordon, H. Kim, N. Salovich, R.W. Giannetta, R.M. Fernandes, V.G. Kogan, T. Prozorov, S.L. Bud'ko, P.C. Canfield, M.A. Tanatar, R. Prozorov, Phys. Rev. B 82 (2010) 054507-054512.
[30] D. Deaumling, D. Larbalastier Phys. Rev. B **40** (1989) 9350-; L. Conner, A.P. Malozemof, Phys. Rev. B 43 (1991) 402-407.
[31] L. Civale, L. Krusin-Elbaum, J.R. Thompson, F. Holtzberg. Phys. Rev B 50 (1994) 7188-7191.
[32] C.J. van der Beek, M. Konczykowski, A. Abal'oshev, I. Abal'osheva, P. Gierlowski, S. J. Lewandowski, M.V. Indenbom, S. Barbanera, Phys. Rev. B 66 (2002) 024523-024533.
[33] N. Haberkorn *et al.* Phys. Rev. B **85** (2012) 174504-174510.
[34] Jeehoon Kim, N. Haberkorn, K. Gofryk, M.J. Graf, F. Ronning, A.S. Sefat, R. Movshovich, L. Civale. Solid State Comm. 201 (2015) 20-24.
[35] J.T. Park *et al.*, Phys. Rev. Lett 102 (2009) 117006-117009.
[36] W.K. Yeoh *et al.*, Phys. Rev. Lett 106 (2011) 247002-247005.
[37] M.P. Maley, J.O. Willis, H. Lessure, M.E. McHenry, Phys. Rev. B 42 (1990) 2639-2642.
[38] J.R. Thompson, L. Krusin-Elbaum, L. Civale, G. Blatter, C. Feild, Phys. Rev Lett. 78 (1997) 3181-3184.
[39] M. Konczykowski, Physica C 209 (1993) 247-250.

Highlights

- Vortex dynamics for a $BaFe_{2-x}Ru_xAs_2$ ($x \approx 0.7$) single crystal is reported.

- J_c at low magnetic fields is well explained by low density of strong pinning centers.

- The collective pinning energy and the glassy μ exponent were estimated.

Figure 1

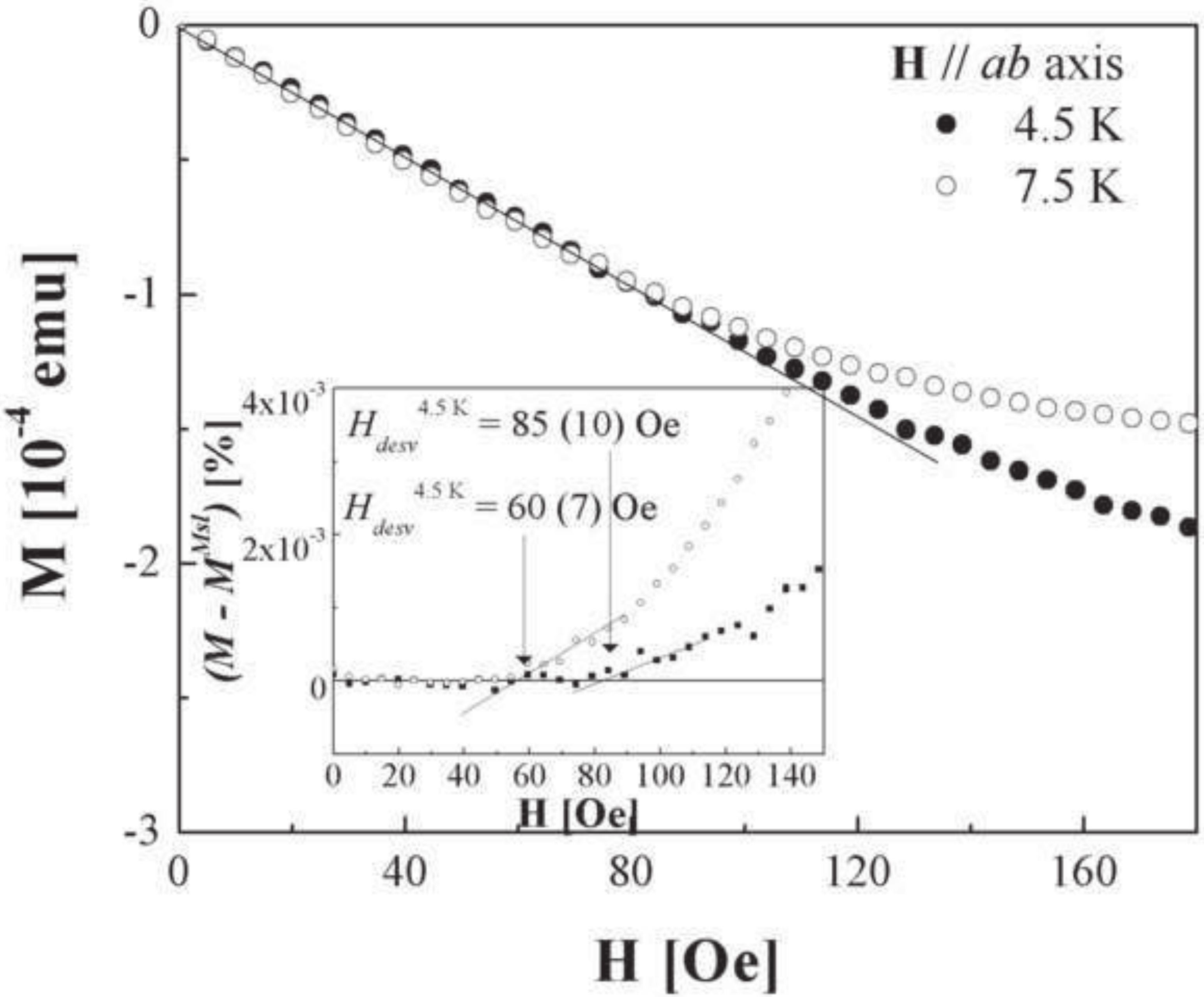

H // ab axis
4.5 K
7.5 K
M [10^-4 emu]
H [Oe]
0
-1
-2
-3
0
40
80
120
160
H_desv 4.5 K = 85 (10) Oe
H_desv 4.5 K = 60 (7) Oe
(M - M^Msl) [%]
4x10^-3
2x10^-3
0
0
20
40
60
80
100
120
140
H [Oe]

Figure 2a

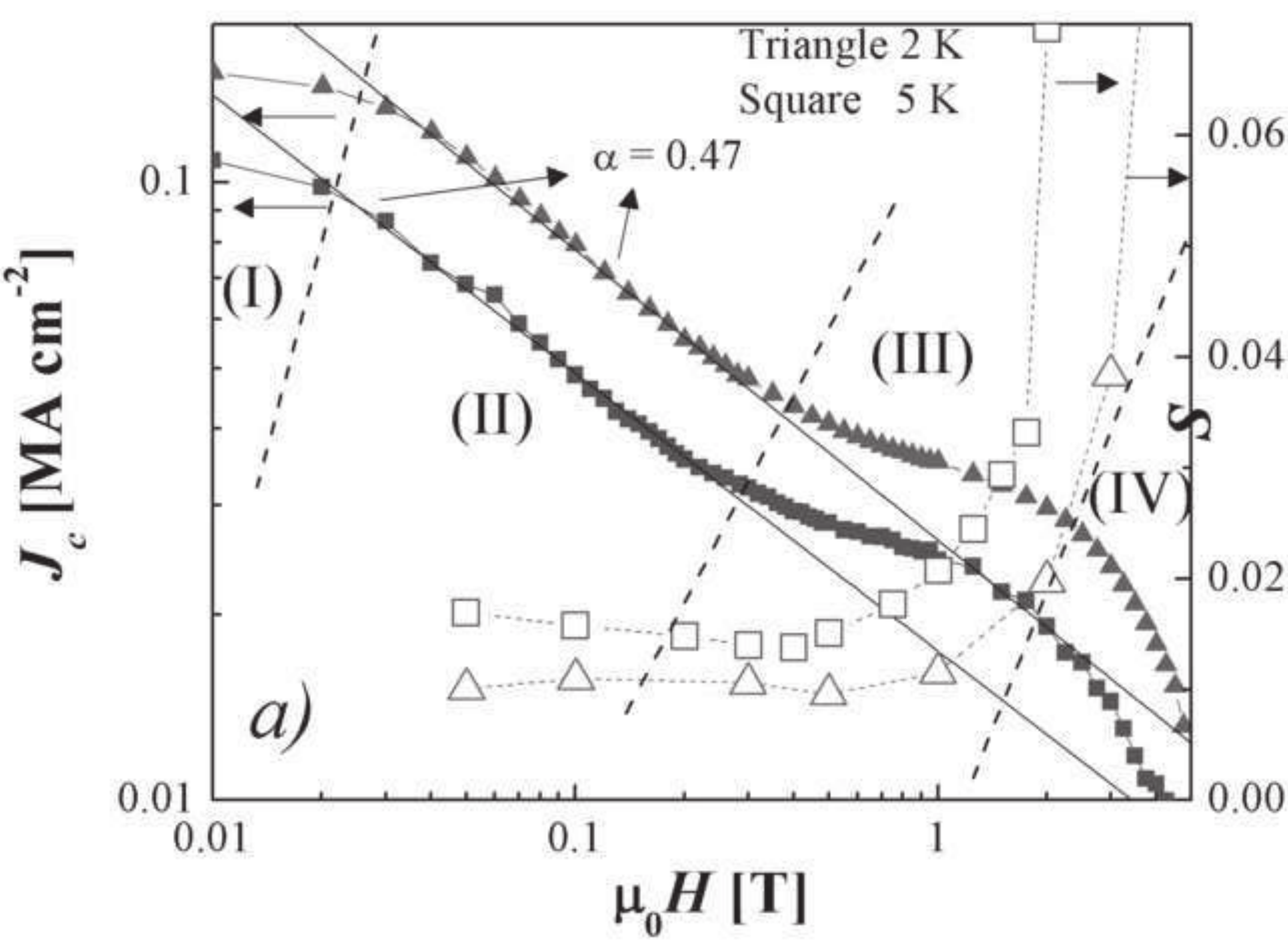

Triangle 2 K
Square 5 K
α = 0.47
(I)
(II)
(III)
(IV)
a)
0.1
0.01
0.01
0.1
1
0.06
0.04
0.02
0.00
J_c [MA cm^{-2}]
$\mu_0 H$ [T]
S

Figure 2b

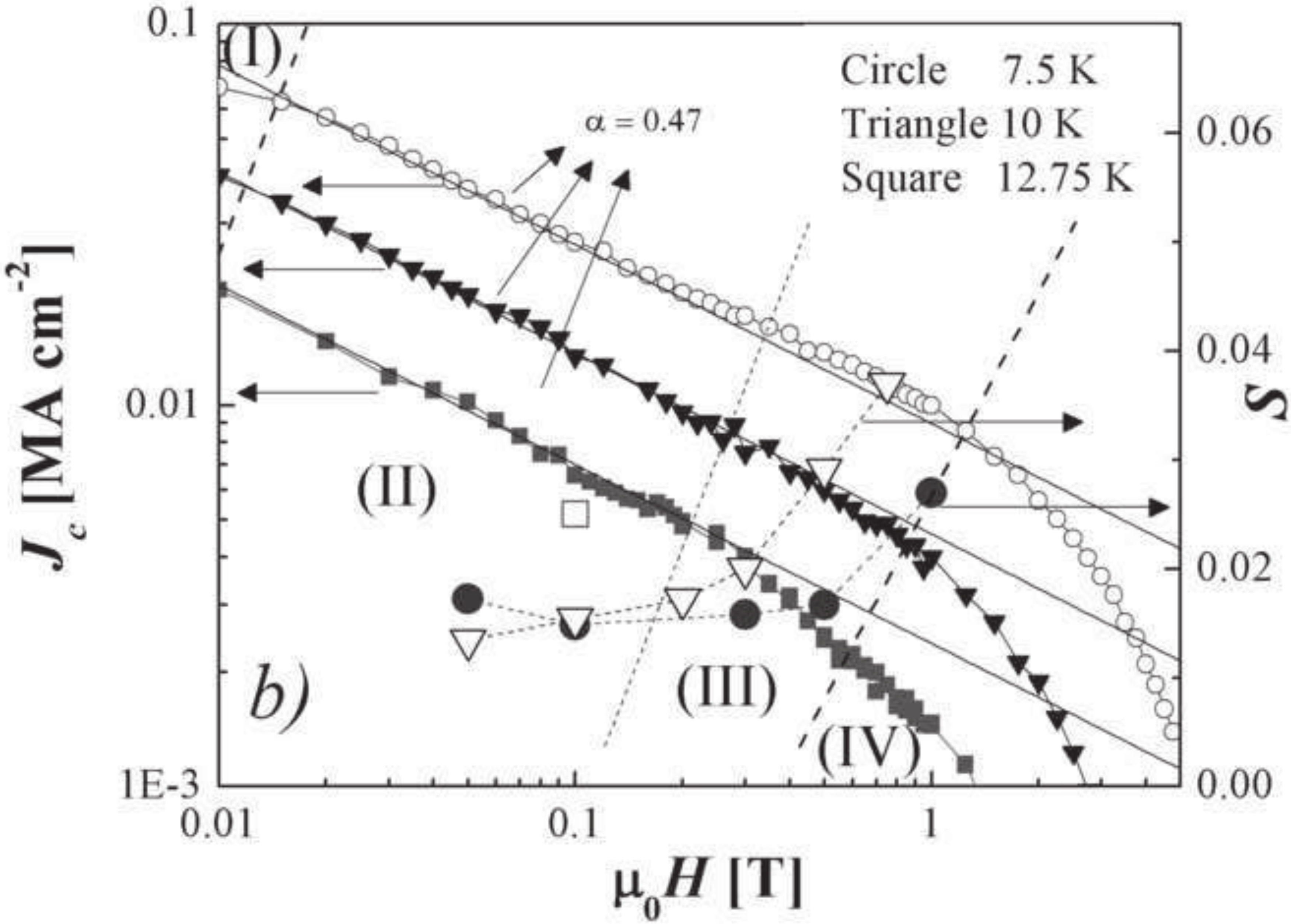

(I)
(II)
(III)
(IV)
b)
α = 0.47
Circle 7.5 K
Triangle 10 K
Square 12.75 K
0.1
0.01
1E-3
0.01
0.1
1
0.06
0.04
0.02
0.00
J_c [MA cm^{-2}]
$\mu_0 H$ [T]
S

Figure 3

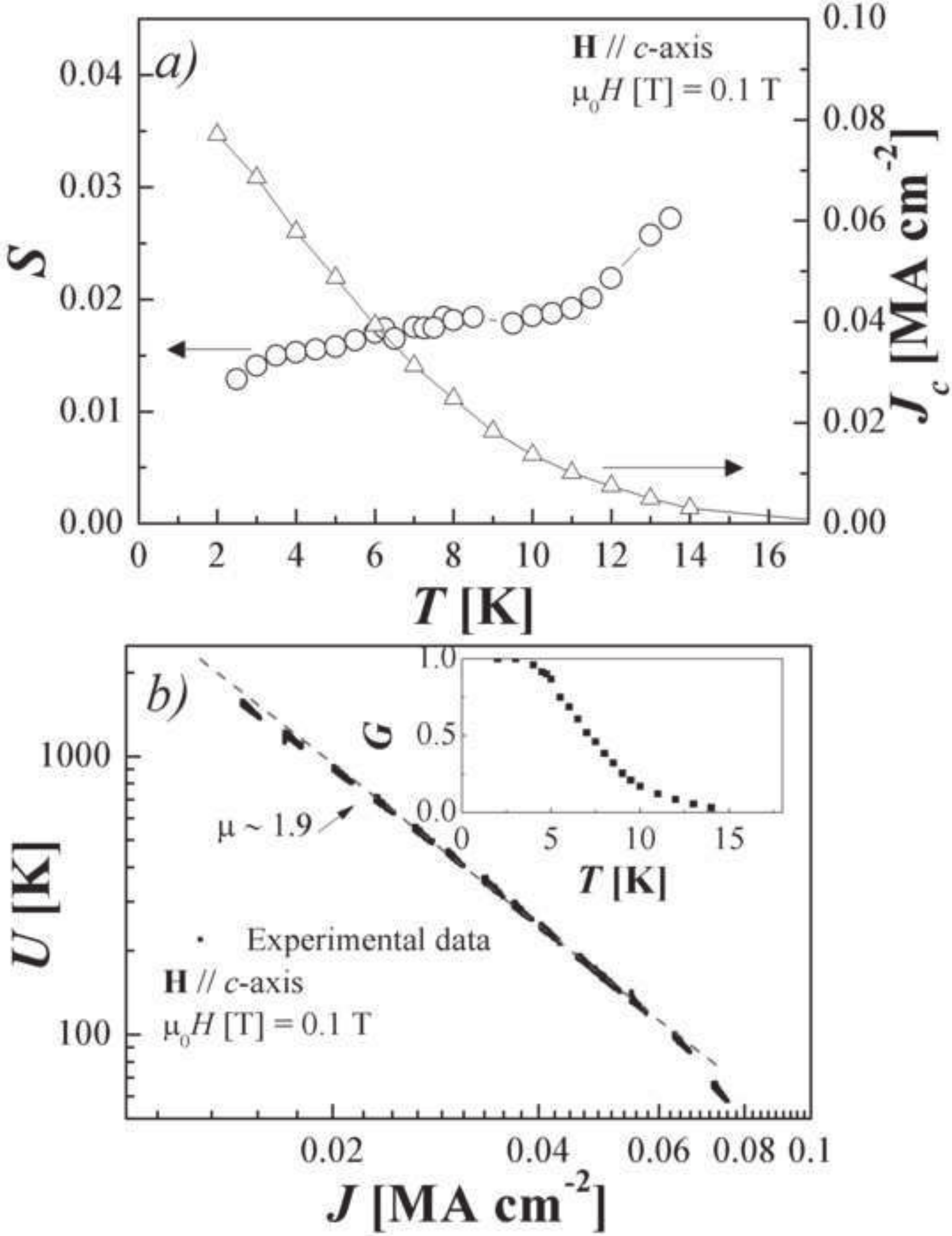

a)
H // c-axis
μ0H [T] = 0.1 T
S
0.00
0.01
0.02
0.03
0.04
Jc [MA cm-2]
0.00
0.02
0.04
0.06
0.08
0.10
0
2
4
6
8
10
12
14
16
T [K]
b)
U [K]
1000
100
μ ~ 1.9
Experimental data
H // c-axis
μ0H [T] = 0.1 T
0.02
0.04
0.06
0.08
0.1
J [MA cm-2]
G
1.0
0.5
0.0
0
5
10
15
T [K]

Figure 4

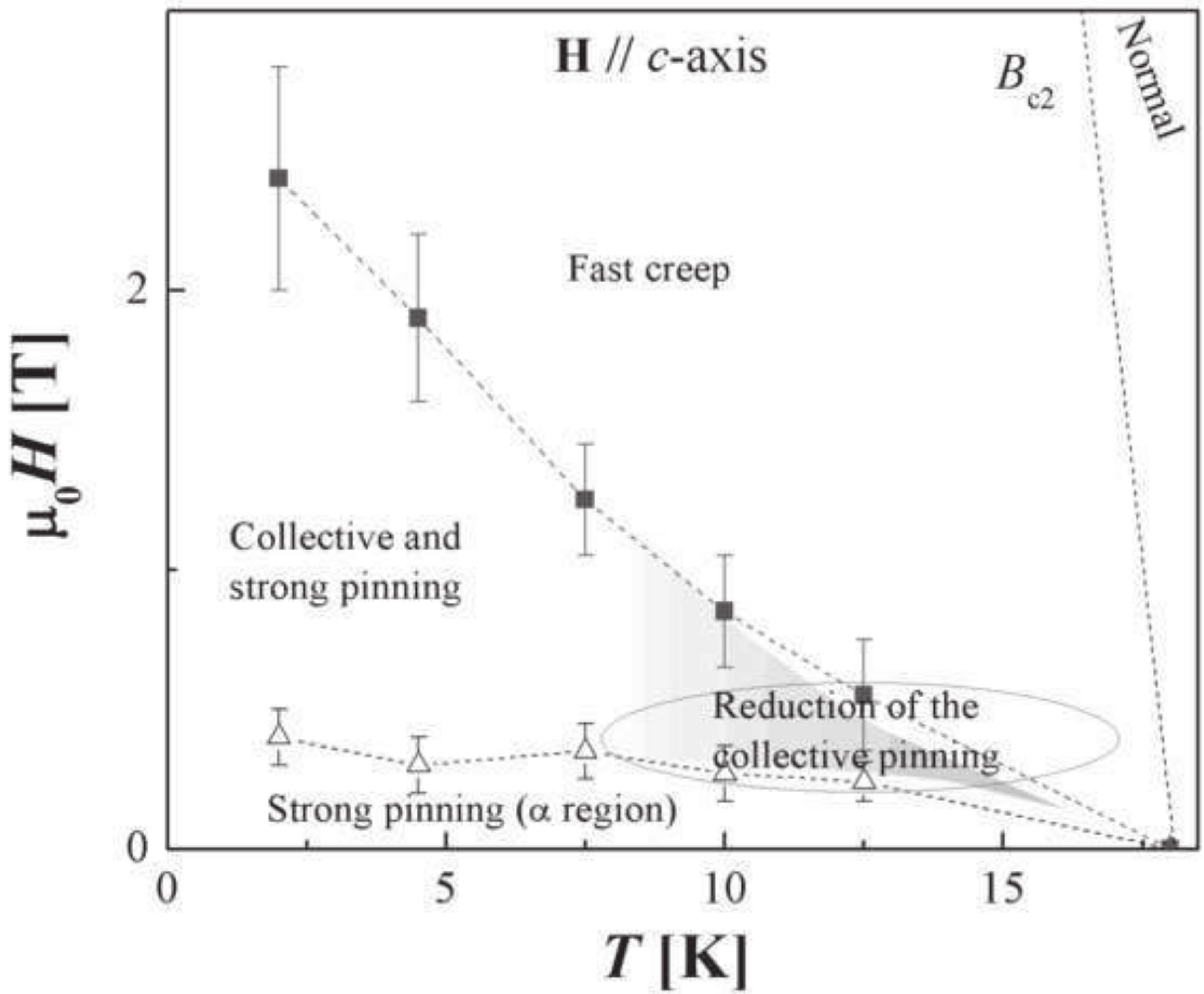
H // c-axis
B_{c2}
Normal
Fast creep
Collective and
strong pinning
Reduction of the
collective pinning
Strong pinning (α region)
2
0
0
5
10
15
$\mu_0 H$ [T]
T [K]